Available online at www.sciencedirect.com
ScienceDirect
Journal of Nuclear Materials 376 (2008) 1–10
journal of nuclear materials
www.elsevier.com/locate/jnucmat

Extension of the TRANSURANUS burn-up model

A. Schubert [a,*], P. Van Uffelen [a], J. van de Laar [a], C.T. Walker [a], W. Haeck [b]

[a] European Commission, Joint Research Centre, Institute for Transuranium Elements, P.O. Box 2340, D-76125 Karlsruhe, Germany
[b] Institut de Radioprotection et de Sûreté Nucléaire, BP 17, F-92262 Fontenay-aux-Roses cedex, France

Received 7 September 2007

Abstract

The validation range of the model in the TRANSURANUS fuel performance code for calculating the radial power density and burn-up in UO_2 fuel has been extended from 64 MWd/kgHM up to 102 MWd/kgHM, thereby improving also its precision. In addition, the first verification of calculations with post-irradiation examination data is reported for LWR-MOX fuel with a rod average burn-up up to 45 MWd/kgHM. The extension covers the inclusion of new isotopes in order to account for the production of ^{238}Pu. The corresponding one-group cross-sections used in the equations rely on results obtained with ALEPH, a new Monte Carlo burn-up code. The experimental verification is based on electron probe microanalysis (EPMA) and on secondary ion mass spectrometry (SIMS) as well as radiochemical data of fuel irradiated in commercial power plants. The deviations are quantified in terms of frequency distributions of the relative errors. The relative errors on the burn-up distributions in both fuel types remain below 12%, corresponding to the experimental scatter.
© 2008 Published by Elsevier B.V.

PACS: 28.41.Ak

1. Introduction

In order to ensure the safe and economic operation of nuclear fuel rods, it is necessary to be able to predict their behaviour and life-time. The accurate description of the fuel rod behaviour, however, involves various disciplines. The strong interrelationship between disciplines calls for the development of computer codes describing the general fuel behaviour. Fuel designers and safety authorities rely heavily on these type of codes since they require minimal costs in comparison with the costs of an unexpected fuel rod failure.

With the steady increase in the discharge burn-up in nuclear power plants beyond 50 MWd/kgHM, codes have been updated. The first step towards increasing the burn-up range of a code consists in adapting the model for the radial power distribution. Indeed, the power density provides the source term for the temperature calculation, affecting most mechanisms in the code, as well as the source term for the radioactive fission products.

However, rather than solving the Boltzmann transport equation like in the WIMS [1,2] or HELIOS [3,4] lattice reactor physics codes which are in use by the nuclear industry in fuel management calculations for nuclear power reactors, fuel performance codes must make use of simpler models for the sake of calculation time. Most of them were derived from the RADAR model [5], which is based on thermal neutron diffusion theory and was validated with WIMS calculations. The original TUBRNP [6] model for power and burn-up calculations included in the TRANSURANUS fuel performance code [7], and later also in other codes like FRAPCON3 [8], extended the RADAR model by including higher Pu isotopes, and modifying the radial shape function that accounts for resonance absorption by ^{238}U. TUBRNP was originally validated for UO_2 fuel in light-water reactors (LWRs) with experimental data from fuel with burn-up values between 35 and 64 MWd/kgHM. Later on, the RAPID model [9]

* Corresponding author. Tel.: +49 7247 951 406; fax: +49 7247 951 99406.
E-mail address: Amdt.Schubert@ec.europa.eu (A. Schubert).

0022-3115/$ - see front matter © 2008 Published by Elsevier B.V.
doi:10.1016/j.jnucmat.2008.01.006

was developed for the COSMOS code [10–12], PLUTON [13] was developed for the FEMAXI code [14], while a specific burn-up model for the RTOP code [15] was developed for fuel rods in Russian-type WWER reactors. RAPID was validated purely on the basis of profiles calculated by HELIOS up to 150 MWd/kgHM, while the others were validated against experimental data up to 83 MWd/kgHM.

A first attempt to compare TUBRNP predictions with electron probe microanalysis (EPMA) data for UO_2, irradiated up to 102 MWd/kgHM in a commercial pressurized-water reactor (PWR), revealed that the pellet-averaged Pu content was under-predicted by roughly 20% [16]. The main objective of the present paper is therefore to explain how the predictive capabilities of the TUBRNP routine were improved, and as such its verification range for UO_2 extended from 64 MWd/kgHM to 102 MWd/kgHM. This is described in the second section of the paper. Another objective of the paper is to analyse for the first time the TUBRNP simulations for commercial $(U,Pu)O_2$ – referred to as mixed-oxide (MOX) fuel – used in LWRs. For LWR-MOX fuel with a burn-up of 45 MWd/kgHM comparisons are made with EPMA and secondary ion mass spectrometry (SIMS) data. The verification of TUBRNP with post-irradiation data is presented and discussed in the third section of the paper. In the fourth and final section of the paper we will summarize the outcome, and outline the perspectives.

2. Extension of the TUBRNP model

The TUBRNP model [6] is based on the proportionality of the local power density, $q'''(r)$, to the neutron flux, $\Phi(r)$, to the concentrations of the relevant isotopes, $N_k(r)$, and to the corresponding one-group fission cross-sections, $\sigma_{f,k}$, that are averaged over the neutron spectrum

$$q'''(r) \propto \sum_k \sigma_{f,k} N_k(r) \Phi(r). \tag{1}$$

The modelling of the radial power profiles is hence split into (a) the approximation of the neutron flux through thermal diffusion theory and (b) the computation of the local concentrations of the relevant actinide isotopes that are either fissile or fertile.

When comparing the predictions of TUBRNP with radiochemical and EPMA data for UO_2 fuel irradiated in a commercial PWR up to a burn-up of 102 MWd/kgHM [17,18], the average Pu content in the fuel section analysed was under-predicted by 20%. In line with the models included in the RTOP code and COSMOS code, it was considered coping with this deviation by introducing the burn-up (or time) dependence in the model parameters. Therefore, the one-group cross-sections should be derived as a function of burn-up on the basis of detailed neutronic calculations. To this end, we adopted the new and more efficient Monte Carlo burn-up code ALEPH [19], which combines the ORIGEN 2.2 isotope depletion code with any version of MCNP or MCNPX for reaction rate calculations. These calculations revealed, however, that rather than upgrading the TUBRNP parameters by making them burn-up dependent, a more physical and simple improvement was needed. It consisted of accounting for the ^{238}Pu production in TUBRNP, since ALEPH calculations showed that the production of this isotope becomes relevant in the burn-up range under consideration. As a result, we have extended the TUBRNP model by including the local concentrations of the isotopes ^{236}U, ^{237}Np, and ^{238}Pu. It now covers the following set of equations:

$$\begin{aligned}
\frac{dN_{U235}(r)}{dbu} &= -\sigma_{a,U235} N_{U235}(r) A,\\
\frac{dN_{U236}(r)}{dbu} &= -\sigma_{a,U236} N_{U236}(r) A + \sigma_{c,U235} N_{U235}(r) A,\\
\frac{dN_{Np237}(r)}{dbu} &= -\sigma_{a,Np237} N_{Np237}(r) A + \sigma_{c,U236} N_{U236}(r) A,\\
\frac{dN_{U238}(r)}{dbu} &= -\sigma_{a,U238} N_{U238}(r) f_{U238}(r) A,\\
\frac{dN_{Pu238}(r)}{dbu} &= -\sigma_{a,Pu238} N_{Pu238}(r) A + \sigma_{c,Np237} N_{Np237}(r) A,\\
\frac{dN_{Pu239}(r)}{dbu} &= -\sigma_{a,Pu239} N_{Pu239}(r) A + \sigma_{c,U238} N_{U238}(r) f_{U238}(r) A,\\
\frac{dN_{Pu240}(r)}{dbu} &= -\sigma_{a,Pu240} N_{Pu240}(r) f_{Pu240}(r) A + \sigma_{c,Pu239} N_{Pu239}(r) A,\\
\frac{dN_{Pu241}(r)}{dbu} &= -\sigma_{a,Pu241} N_{Pu241}(r) A + \sigma_{c,Pu240} N_{Pu240}(r) f_{Pu240}(r) A,\\
\frac{dN_{Pu242}(r)}{dbu} &= -\sigma_{a,Pu242} N_{Pu242}(r) A + \sigma_{c,Pu241} N_{Pu241}(r) A.
\end{aligned} \tag{2}$$

Here $N_j(r)$ is the local concentration of the isotope j, σ_a and σ_c are the one-group effective cross-sections for total neutron absorption and neutron capture, respectively, and 'A' is a conversion constant (see [6] for details). This evaluation assumes a quasi-immediate β-decay of ^{237}U and ^{238}Np analogous to modelling the generation of ^{239}Pu by neutron capture of ^{238}U and quasi-immediate β-decay of ^{239}U and ^{239}Np.

In line with the original TUBRNP model, a radial form factor $f(r)$ is used to account for the strong absorption of resonance neutrons in ^{238}U and ^{240}Pu

$$f(r) = 1 + p_1 \exp\left(-p_2 (R - r)^{p_3}\right), \tag{3}$$

where R is the fuel outer radius. The constants p_1, p_2 and p_3 had been derived after comprehensive comparisons with measurements of fuel slices irradiated in LWRs [6] as well as in the Halden HWR [20]. While p_1 differs between LWRs ($p_1 = 3.45$) and the Halden HWR ($p_1 = 2.21$), the values $p_2 = 3.0$ and $p_3 = 0.45$ hold for both reactor types. Owing to the asymptotic behaviour of expression (3) at the minimum and maximum pellet radii, the main parameter p_1 can be interpreted as an estimate of the ratio of integrals for resonance and thermal neutrons

$$p_1 \approx \frac{\int_{res} \sigma_c(E) \Phi(E)\, dE}{\int_{th} \sigma_c(E) \Phi(E)\, dE}, \tag{4}$$

where $\sigma_c(E)$ is the differential neutron capture cross-section and $\Phi(E)$ denotes the neutron flux per energy.

For the present update of TUBRNP, the reaction parameters in the equation sets (2) and (4) have been refined as follows. First of all, updated one-group effective cross-sections have been inferred from calculations with the SCALE 4.4 code package [21]. Specific cross-sections were derived for both UO_2 and MOX fuel: This was necessary because due to the different initial composition between UO_2 and MOX and the concomitant different neutron spectrum, one observes in MOX fuel a larger flux depression at begin-of-life and a higher Pu content in the pellet centre at end-of-life. These differences have been accounted for in the present TUBRNP model by applying dedicated one-group cross-sections, treating all U and Pu isotope concentrations locally, and including the resonance capture of ^{240}Pu by a specific radial form factor $f_{Pu240}(r)$. Its radial dependence is treated analogously to that in ^{238}U (3), as only difference a specific parameter $p_1(^{240}\mathrm{Pu})$ is applied. Based on relation (3) it has been estimated as follows:

$$\frac{p_1(^{240}\mathrm{Pu})}{p_1(^{238}\mathrm{U})} = \frac{\mathrm{RI}(^{240}\mathrm{Pu})}{\sigma_{c,th}(^{240}\mathrm{Pu})}\,\frac{\sigma_{c,th}(^{238}\mathrm{U})}{\mathrm{RI}(^{238}\mathrm{U})} = 0.28, \tag{5}$$

where RI are the resonance integrals and $\sigma_{c,th}$ are the thermal neutron capture cross-sections of the given isotopes. The values are compiled in Table 1 and have been taken from Refs. [22,23] and a recent re-analysis of the thermal neutron capture cross-section in ^{238}U [24].

To give a complete account of the total Pu concentration, an additional component for generation of ^{238}Pu is calculated from α-decay of ^{242}Cm. To this end we have not further extended the set of Eq. (2) but applied a recursive analytical algorithm as outlined in Ref. [25], describing the build-up of the isotope chain starting from ^{241}Pu. This chain is illustrated in Fig. 1 together with the build-up of ^{238}Pu from ^{235}U according to equation set (2). However, no experimental data are at present available for a separate verification of the concentration of these specific isotopes.

Table 1
Resonance integrals (RI) and thermal neutron capture cross-sections ($\sigma_{c,th}$) of the isotopes ^{238}U and ^{240}Pu

	^{238}U	^{240}Pu
RI	277 b	8450 b
$\sigma_{c,th}$	2.68 b	290 b

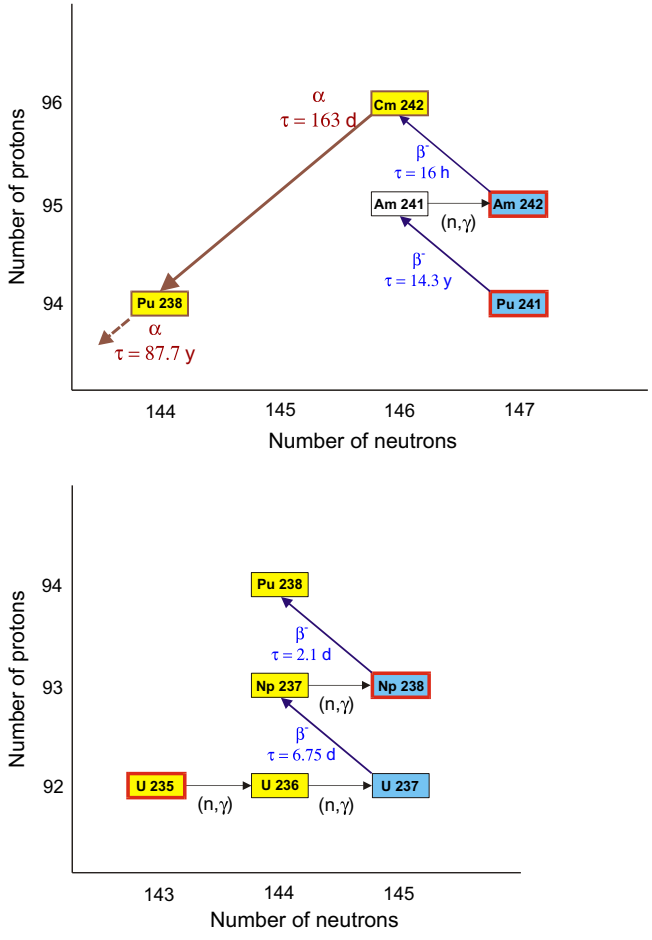

Fig. 1. Scheme describing the isotope chains for build-up of ^{238}Pu implemented in the new version of TUBRNP.

3. The experimental data for the verification

Burn-up models are usually compared with microscopic experimental data of irradiated nuclear fuels. In the present paper we combine wavelength dispersive electron probe microanalysis (EPMA) performed at ITU Karlsruhe [17,26] for local element concentrations, and SIMS [27–30] performed at the Paul Scherrer Institute, Switzerland, for local isotope concentrations. A radiochemical assessment of the total Pu content in the fuel was used as well [17]. For EPMA of plutonium a PuO_2 standard was employed and for fission product neodymium a Nd metal standard was used. A detailed description of the approach used for the determination of the corresponding radial distributions together with estimates of the accuracy can be found in Ref. [20] for UO_2 fuel and in Ref. [31] for LWR-MOX fuel. When comparing TUBRNP computations with EPMA results, it is assumed that the normalized distribution of local burn-up is identical to that of the local Nd concentration.

The most important characteristics of the irradiated fuel samples are listed in Table 2, while more details about the irradiation history and experimental techniques have been published earlier [17,18]. All samples are related to fuel used in LWRs. For MOX fuel the sub-types SBR (short-binderless route), MIMAS (micronized master-blend) and OCOM (optimized co-milling) correspond to three different fuel production technologies, resulting in different levels of homogeneity (see e.g. Ref. [31] for further information).

Table 2
Main characteristics of the fuels used in LWRs for extending the verification of TUBRNP

Fuel type	Sample		Radius (mm)	Initial concentration $^{235}U/^{tot}U$ (wt%)	Slice-average burn-up (MWd/kgHM)	Refs.
	#	ID				
UO_2 LWR	1	Regate L10/4009S3	4.096	4.5	49.5	[38,39]
	2	12C3-LP			69	
	3	12H3-HP	4.65	3.5	95	[17,26]
	4	12C3-HP			102	
MOX SBR	5	CT12 (5.54% Pu)	4.645	0.30	33.6	[31]
MOX OCOM	6	OCOM30 (5.07% Pu)	4.565	0.72	44.5	[35]
MOX MIMAS	7	5784 (10.11% Pu)	4.02	0.58	34	[29,30]

The sub-types SBR, OCOM and MIMAS correspond to different production technologies of LWR-MOX, see text for details.

4. Verification of the TUBRNP model

4.1. Average Pu concentrations

Fig. 2 shows radially averaged Pu concentrations measured by EPMA for irradiated slices of UO_2 fuel and compares them with the predictions of the TUBRNP model.

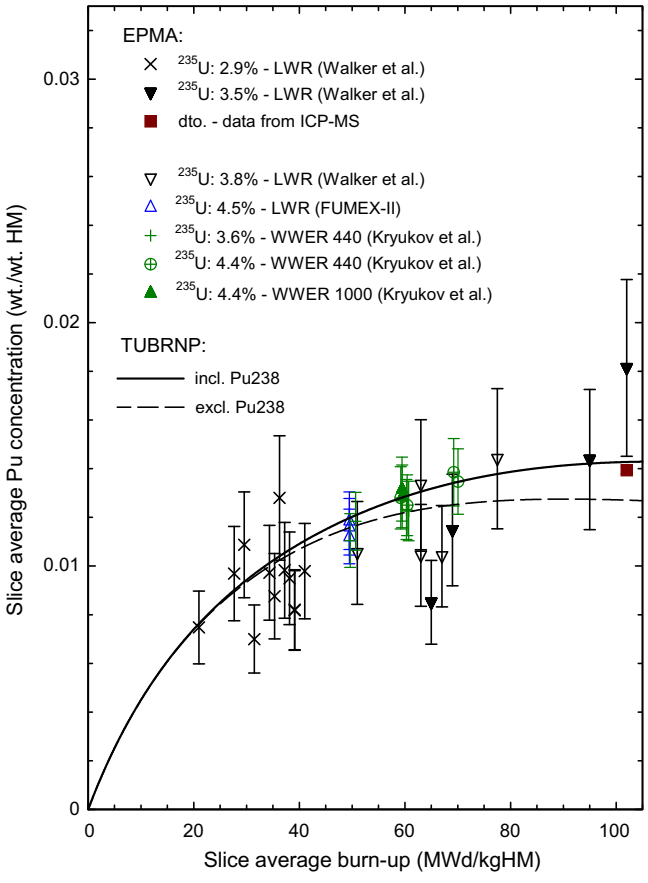

Fig. 2. Slice-average total plutonium concentration as calculated by TRANSURANUS compared with EPMA measurements of irradiated UO_2 fuel. The data for an initial ^{235}U concentration of 2.9% are taken from Refs. [6,26]. The samples with an initial ^{235}U concentration of 3.5% are described in Ref. [26], those with 3.8% in Refs. [36,37]. The graph is complemented by data from LWR-UO_2 used in the IAEA coordinated research project FUMEX-II [38], and by data from WWER fuel [32].

The graph includes data from earlier measurements that were used for establishing the TUBRNP model [6], as well as data published for Russian-type WWER fuel [32]. For all EPMA measurements performed at ITU, an estimated error of the absolute Pu concentration of ±20% is marked. For the remaining measurements an overall error of ±10% is assumed.

On the basis of the results in Fig. 2, one can conclude that the agreement between measured and calculated values is very satisfactory, when considering the scatter in the available experimental data. It is similar to that observed previously for intermediate burn-up LWR-UO_2 fuel [6], Furthermore, the data do not show any difference between the trends for LWR and WWER fuels.

The results in Fig. 2 also reveal that the contribution of the ^{238}Pu isotope to the total Pu concentration becomes increasingly important above a slice-averaged burn-up of 60 MWd/kgHM. When extrapolating the trend for TUBRNP beyond 100 MWd/kgHM, further refinements will have to be considered to account for the increasing number of relevant actinide isotopes as in the ALEPH code. One should bear in mind, however, that the primary objective of the TUBRNP model in the fuel performance code consists in predicting the relative radial power distribution, since the linear heat rating or the section-average power density is provided on input. As will be seen in the next sections, predictions of the relative power production in the burn-up range under consideration are even better than the predictions of the absolute Pu concentrations, both for UO_2 and for MOX fuel.

4.2. Radial distributions in UO_2 fuel

In Fig. 3 we compare measured with calculated radial distributions of local burn-up and normalized Pu concentrations for LWR-UO_2 fuel with the highest burn-up level of 102 MWd/kgHM. The agreement between the TUBRNP profiles and both the experimental profile as well as the profiles provided by the detailed neutronic computations with ALEPH is very good. Despite the assumptions on the power history and irradiation conditions that had to be made for the ALEPH computations [16], the radial profiles appear to be well predicted even with

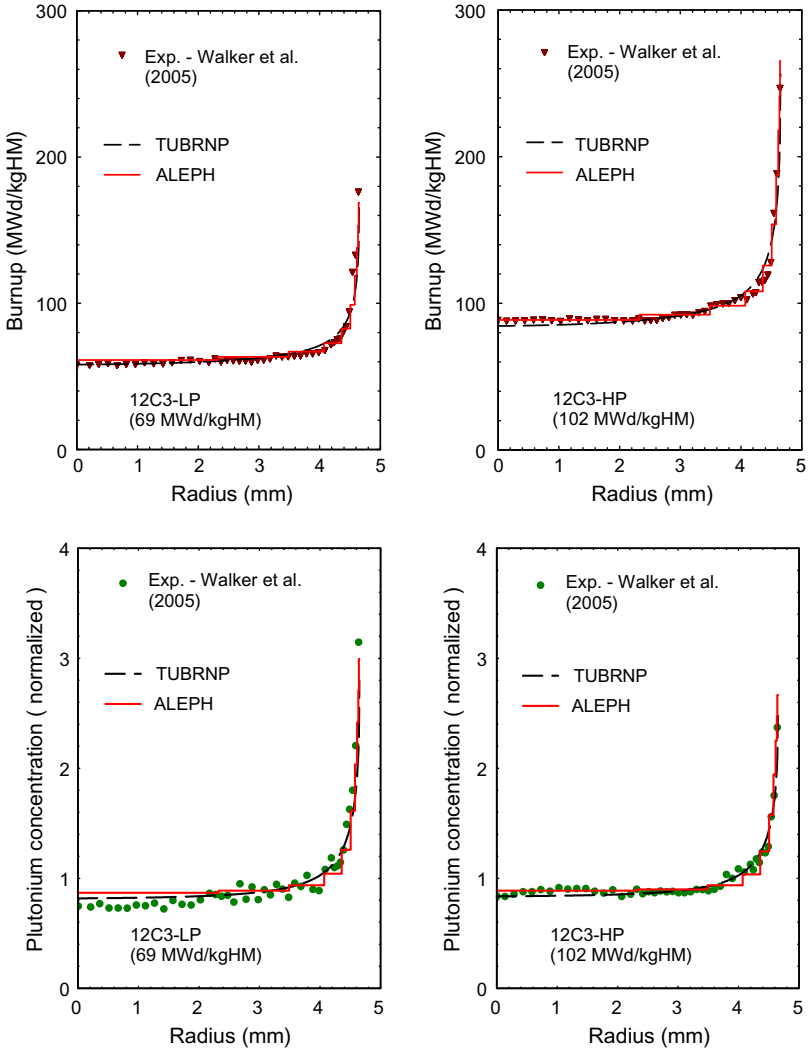

Fig. 3. Radial distribution of the local burn-up (top) and the normalized Pu content (bottom) calculated by TUBRNP and compared with EPMA measurements for samples #2 and #4 [17,26] at high burn-up.

the simple geometrical model used. A sensitivity study of the power history has been carried out with ALEPH revealing no significant deviations in the results. It was concluded that the normalized radial distributions of both Pu and Nd are dependent on the final burn-up, but are rather independent of how the burn-up was accumulated [16]. This observation is consistent with the good agreement between the radial Pu and burn-up profiles calculated by TUBRNP and the experimental data, despite of the independence of TUBRNP on the path of burn-up accumulation.

Fig. 4 summarizes the measured and calculated quantities of the local burn-up and the absolute Pu concentration (i.e. not normalized) for all experimental data considered. The histograms on the right-hand side of Fig. 4 contain the probability distributions of the relative differences between the calculated (C) and measured (E) values, together with the number of data points analysed (N), and the root of the mean-square difference

$$s = \sqrt{\frac{1}{N}\sum_{i=1}^{N}\left(\frac{C_i - E_i}{E_i}\right)^2}. \quad (6)$$

For the predictions of TUBRNP, the above defined root of the mean-square difference is 11.5% and 14.6% of the experimental value of burn-up and Pu, respectively, which is the order of magnitude of the experimental errors. This quantity corresponds to the entire range of data, where the largest deviations are observed for the lower and medium range of burn-up and plutonium values. It is therefore fair to conclude that the verification range of TUBRNP has been extended from 64 MWd/kgHM to 102 MWd/kgHM without loss of accuracy.

For an exact quantitative comparison between calculation and experiment, the calculated radial profiles have to be integrated over the final probe diameter of the EPMA measurement. A mean value of 3.5 μm is applied in our case, and a sensitivity test revealed that the impact is

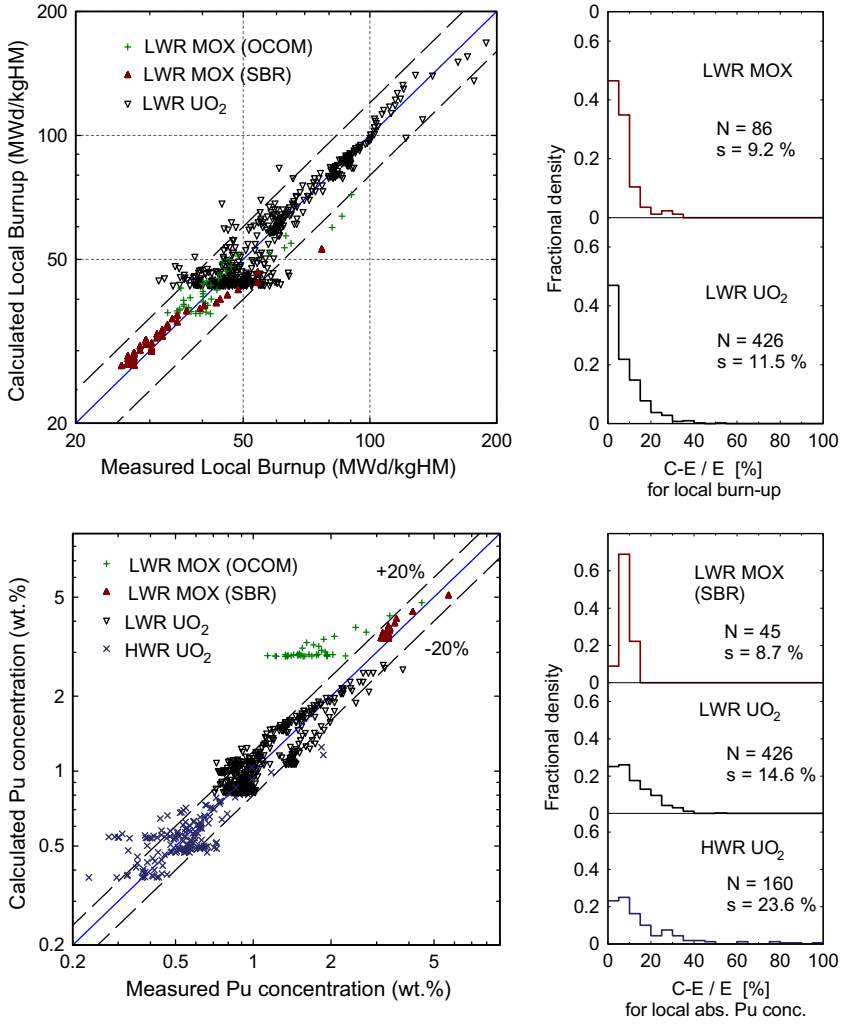

Fig. 4. Comparison of experimental data with values calculated by TUBRNP for the local burn-up (top) and the total Pu content (bottom, including also data for UO_2 irradiated in the Halden HWR [20]). See text for details.

negligible when varying the probe diameter between 0 and 5 μm.

4.3. Radial distributions in MOX fuel

Before considering the radial distributions in MOX fuel, it should be emphasized that the TUBRNP model does not consider variations of the initial U and Pu isotope concentrations across the fuel radius, i.e. any gradients that evolve are solely due to irradiation. Hence, all fuels are implicitly treated as homogeneous materials. Such a treatment is also common practice in detailed neutronic calculations with codes like WIMS or ALEPH.

As a first step in the model verification for MOX, our analysis covers EPMA measurements of irradiated MOX fuel with a high degree of homogeneity, manufactured by the SBR (short-binderless route) process of BNFL [31,33,34]. In addition, the calculations were compared with the non-agglomerate fraction (i.e. corresponding to the initial UO_2 matrix) in irradiated heterogeneous OCOM (optimized co-milling) MOX [35]. As revealed in Fig. 5, for SBR MOX the agreement of the local burn-up calculated by the extended TUBRNP model with that derived from EPMA measurements of Nd is very satisfactory (top), and the agreement of the normalized Pu distributions is excellent (bottom). The situation is very similar for the non-agglomerate part of the OCOM MOX fuel. Although in this case the scatter in the experimental data is much larger, it supports the assumption that modelling the MOX fuel as homogeneous material is appropriate for calculating the radial power profiles in fuel performance calculations.

As a second step in the verification for MOX we have compared in Figs. 6 and 7 computations with SIMS measurements obtained from the PRIMO MOX irradiation programme [28,30]. While the SIMS measurements provide distributions of isotope concentrations over the entire pellet diameter and reveal an asymmetric profile, the TUBRNP computations assume azimuthal symmetry. A good agreement between the calculated and measured normalized concentrations of Pu isotopes is observed. Furthermore, the dashed lines correspond to the results of the previous version of TUBRNP that was not adapted for MOX fuel.

For the present fuel with a high initial Pu content (>10%), the impact of the TUBRNP extension on the radial burn-up distribution is rather small. As expected, a considerable effect can be seen in the radial profiles of ^{240}Pu and ^{241}Pu (Fig. 7), closely linked to the extension of the resonance absorption in ^{240}Pu. It should be noted that the MOX fuel analysed is heterogeneous and has been produced by the MIMAS (micronized master-blend) process [29].

A summary of the relative errors on the profiles predicted by means of TUBRNP for MOX fuel is provided in Fig. 4. Because the MOX-specific extensions of the TUBRNP model do not imply any additional fits of model parameters to experimental data, we should expect larger differences in the absolute (not normalized) total Pu concentrations in different types of irradiated MOX fuel. Nevertheless, except for the samples of the UO_2 matrix in the heterogeneous OCOM MOX, all mean differences are of the order of the experimental uncertainties for the EPMA measurements (up to 20% for determining absolute Pu concentrations).

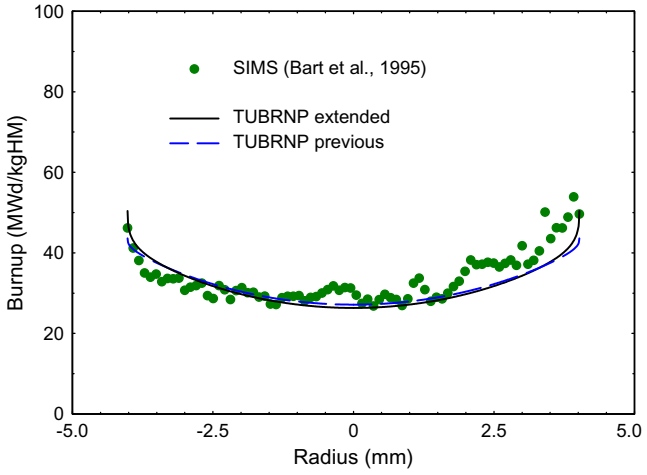

Fig. 6. Radial distribution of the local burn-up in an irradiated MOX sample (#7) at a radially averaged burn-up of 34 MWd/kgHM calculated by TUBRNP compared with SIMS measurements [28,30].

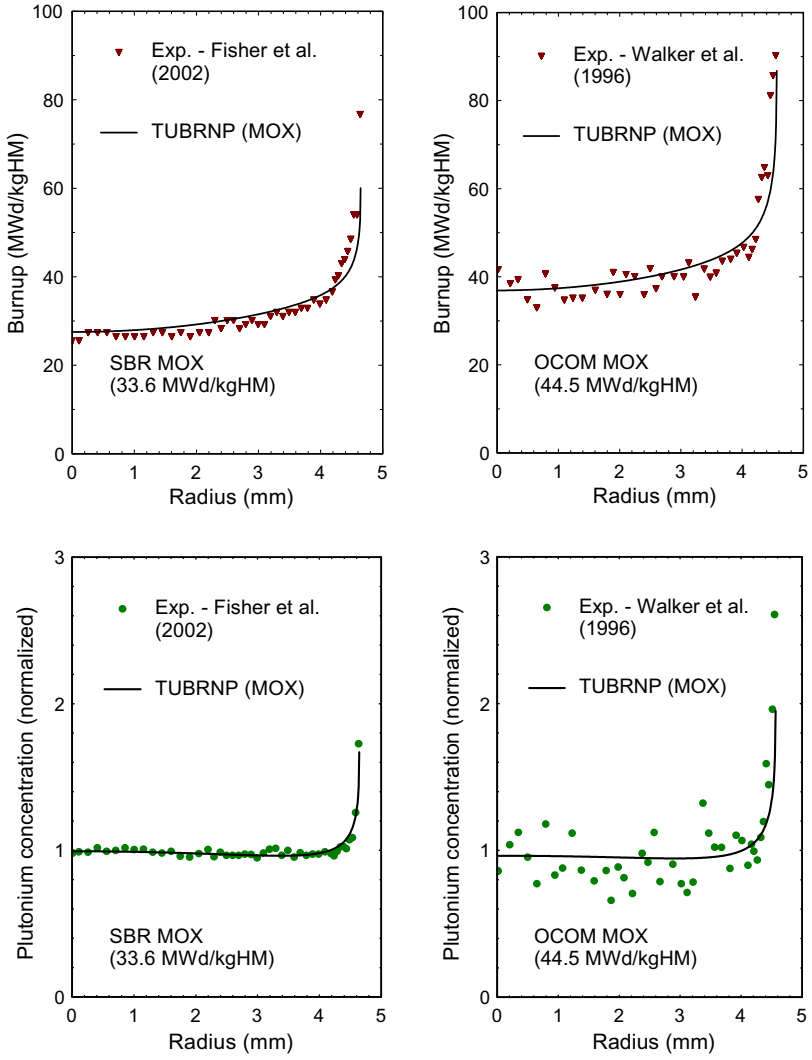

Fig. 5. Radial distribution of the local burn-up (top) and the normalized Pu content (bottom) calculated by TUBRNP and compared with EPMA measurements for samples #5 (SBR MOX [31]) and #6 (OCOM MOX [35]), cf. Table 2.

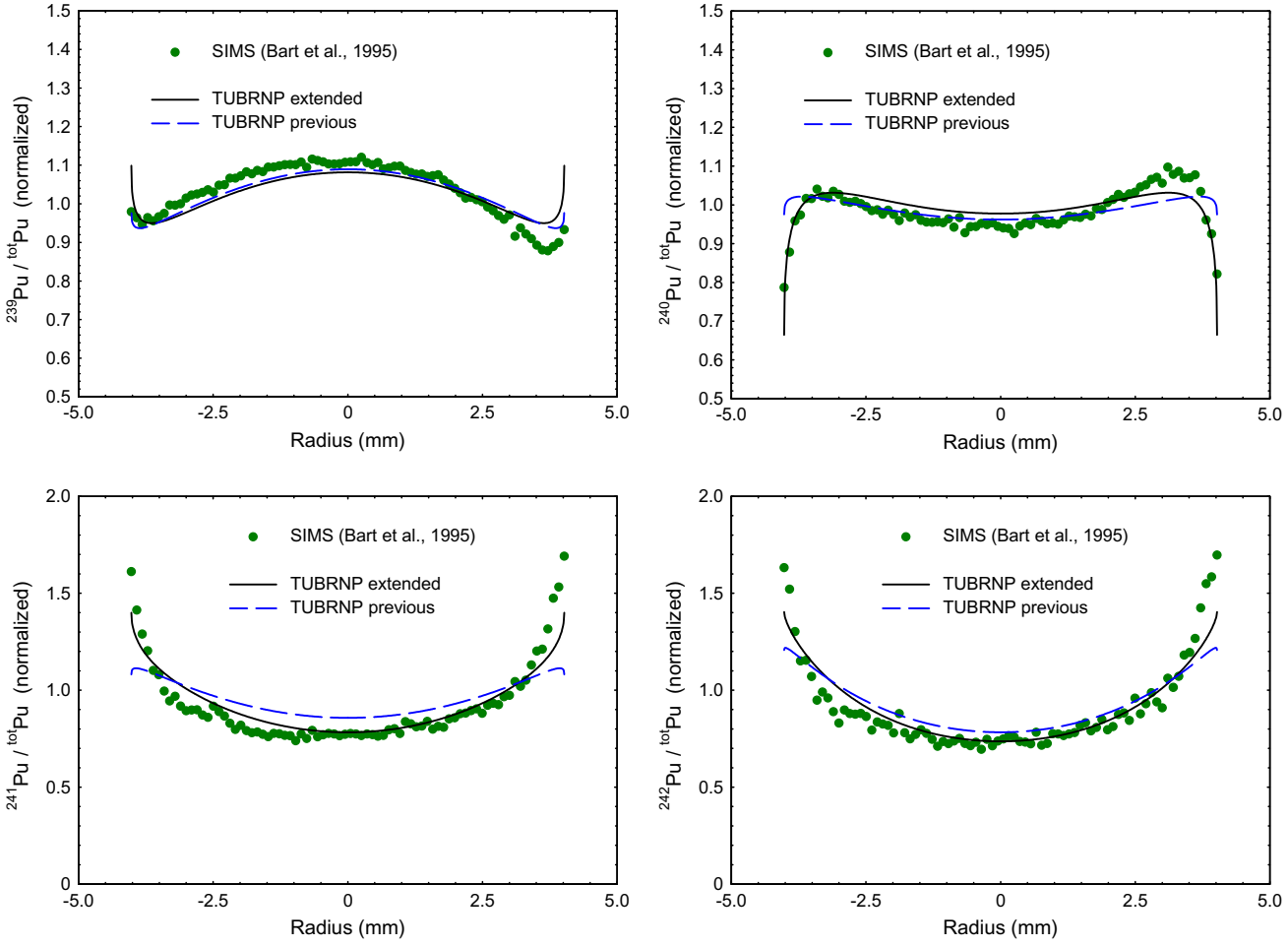

Fig. 7. Radial distribution of the normalized isotope contents of ^{239}Pu, ^{240}Pu, ^{241}Pu and ^{242}Pu in an irradiated MOX sample (#7) at a radially averaged burn-up of 34 MWd/kgHM calculated by TUBRNP compared with SIMS measurements [28,30].

Fig. 4 furthermore compares the present data with those used in Fig. 6 of [20], confirming that the application of TUBRNP to high burn-up UO_2 and MOX fuels does not increase the mean deviations nor introduces any bias.

Finally, the influence of the present extensions of the TUBRNP model on the radial distribution of the local power density, as well as on the fuel centre temperatures calculated by the TRANSURANUS code has been ana-

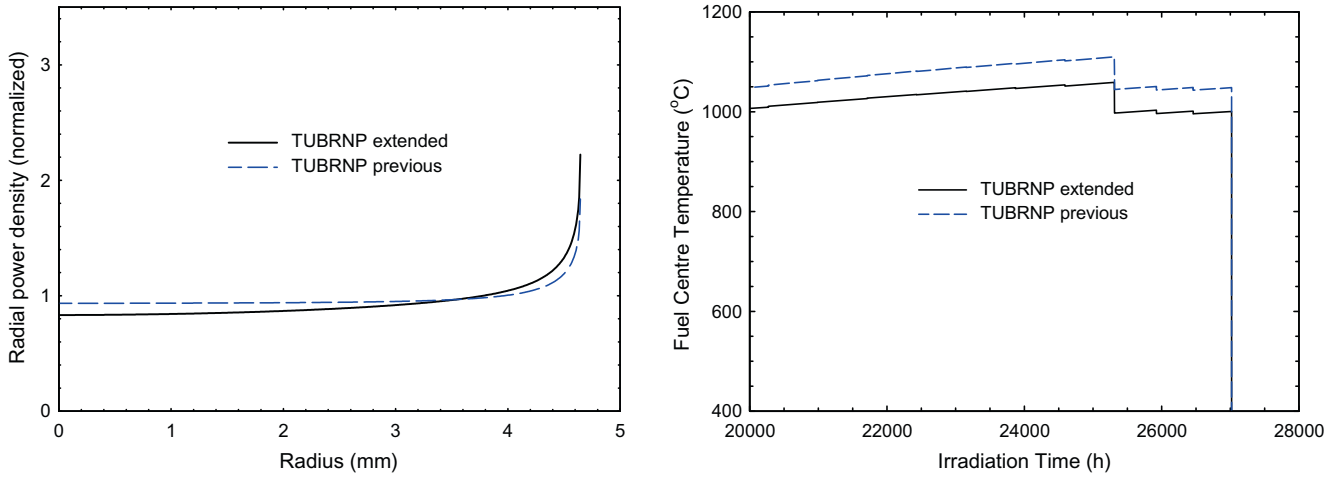

Fig. 8. Comparison of the previous (dashed) and the extended version of TUBRNP (full) for one slice of SBR MOX fuel (sample #5 in Table 2); (a) calculated radial power distribution and (b) fuel centre temperature calculated by TRANSURANUS in the final phase of a real irradiation.

lysed. Fig. 8 shows the calculated radial power profiles at the end of a real irradiation for one slice of SBR MOX fuel in a PWR [34] (sample #5 in Table 2). The shape of the power profiles, hence also the burn-up profiles, is only moderately affected when using the modifications for MOX in TUBRNP (Fig. 8(a)). Nevertheless, the shift of the power profile towards the pellet periphery leads to a measurable decrease of the fuel centre temperature calculated by TRANSURANUS (Fig. 8(b)) up to 50 K. It should be emphasized that the change in fuel central temperature indicated in Fig. 8(b) is only due to the modifications to TUBRNP, i.e. all remaining differences between UO_2 and MOX (e.g. in thermal conductivity) have by purpose been disregarded. The sudden drop in the calculated temperatures is due to the decrease of the linear power applied on input.

5. Summary

We have described the recent extension of the TUBRNP model and its first application to MOX fuel used in LWRs. The verification relies on a comparison with average Pu contents, radial profiles of plutonium isotopes, as well as burn-up profiles obtained by EPMA, SIMS and radiochemical data on irradiated fuel published in the open literature. In addition, the model has been compared with results obtained with the new Monte Carlo burn-up model ALEPH.

For UO_2 fuel, the results confirm that the model is applicable up to a slice-average burn-up around 102 MWd/kgHM. The standard deviation for the relative errors on the absolute Pu concentrations is 15%, which is of the order of the experimental uncertainty and confirms that there has been no loss in precision when extending the burn-up range from 64 to 102 MWd/kgHM. Furthermore, the standard deviations for the normalized plutonium and burn-up profiles (both directly related to the normalized radial power profile the calculation pf which is the main purpose of TUBRNP), are better than 12%. Finally, it was found that the effect of the power history on the shape of these radial profiles is negligible.

For LWR-MOX fuel, our first verification computations of burn-up and plutonium profiles encompassed the SBR, MIMAS and OCOM fuel types with a burn-up range up to 45 MWd/kgHM. The standard deviation for the relative errors on these profiles is approximately 9%. They thus confirm the applicability of the homogenous fuel approximation to the analysed types of MOX, although more data including also higher burn-up fuel is needed to confirm the complete equivalence to UO_2 fuel.

Acknowledgements

The authors gratefully acknowledge K. Lassmann for laying the foundations of the TRANSURANUS code and the TUBRNP model.

References

[1] T.D. Newton, J.L. Hutton, in: M.G. Park (Ed.), Proceedings of PHYSOR 2002 – International Conference on the New Frontiers of Nuclear Technology: Reactor Physics, Safety and High-Performance Computing, 14A-04, American Nuclear Society, Seoul, Korea, 7–10 October 2002, ISBN 0-89448-672-1.
[2] J.L. Hutton, T.D. Newton, R.J. Perry, D.J. Powney, in: Proceedings of PHYSOR 2004 – The Physics of Fuel Cycles and Advanced Nuclear Systems: Global Developments, Session 1D, American Nuclear Society, Chicago, Illinois, USA, 25–29 April 2004, ISBN 0-89448683-7.
[3] R.J.J. Stammler, S. Boerresen, J.J. Casal, P. Forslund, in: Proceedings of PHYSOR 1996 – International Conference on Physics of Reactors, American Nuclear Society, Mito, Ibaraki, Japan, 16–20 September 1996.
[4] HELIOS Methods, Program Manual Rev. 1, Program HELIOS 1.4, Studsvik-Scandpower, 1998.
[5] I.D. Palmer, K.W. Hesketh, P.A. Jackson, in: J. Gittus (Ed.), Water Reactor Fuel Element Performance Computer Modelling, Applied Science, Barking, UK, 1983, p. 321.
[6] K. Lassmann, C. O'Carroll, J. van de Laar, C.T. Walker, J. Nucl. Mater. 208 (1994) 223.
[7] K. Lassmann, J. Nucl. Mater. 188 (1992) 295.
[8] FRAPCON-3: A Computer Code for the Calculation of Steady-State, Thermal-Mechanical Behavior of Oxide Fuel Rods for High Burnup, Report NUREG/CR-6534-V2, (PNNL-11513-V2), December 1997.
[9] C.B. Lee, B.G. Kim, J.S. Song, J.G. Bang, Y.H. Jung, J. Nucl. Mater. 282 (2000) 196.
[10] Y.H. Koo, B.H. Lee, D.S. Sohn, J. Korean Nucl. Soc. 30 (1998) 541.
[11] Y.H. Koo, B.H. Lee, D.S. Sohn, Ann. Nucl. Energy 26 (1999) 47.
[12] B.H. Lee, Y.H. Koo, J.Y. Oh, J.S. Cheon, D.S. Sohn, Nucl. Technol. 157 (2007) 53.
[13] S. Lemehov, J. Nakamura, M. Suzuki, Nucl. Technol. 133 (2001) 153.
[14] M. Suzuki, Nucl. Eng. Des. 201 (2000) 99.
[15] S.Y. Kurchatov, V.V. Likhanskii, A.A. Sorokin, O.V. Khoruzhii, Atom. Energy 92 (2002) 349.
[16] W. Haeck, B. Verboomen, A. Schubert, P. Van Uffelen, Microsc. Microanal. 13 (2007) 179.
[17] C.T. Walker, V.V. Rondinella, D. Papaioannou, S.V. Winckel, W. Goll, R. Manzel, J. Nucl. Mater. 345 (2005) 192.
[18] C.T. Walker, D. Staicu, M. Sheindlin, D. Papaioannou, W. Goll, F. Sontheimer, J. Nucl. Mater. 350 (2006) 19.
[19] W. Haeck, B. Verboomen, Nucl. Sci. Eng. 156 (2007) 180.
[20] K. Lassmann, C.T. Walker, J. van de Laar, J. Nucl. Mater. 255 (1998) 222.
[21] SCALE: A Modular Code System for Performing Standardized Computer Analyses for Licensing Evaluation, NUREG/CR-0200, Rev. 6 (ORNL/NUREG/CSD-2/R6), December 1999.
[22] A.L. Nichols, D.L. Aldama, M. Verpelli, Handbook of Nuclear Data for Safeguards/INDC(NDS)-0502, IAEA – International Nuclear Data Committee, Vienna, 2007.
[23] M.B. Chadwick, P. Oblozinsky, M. Herman, et al., Nucl. Data Sheets 107 (2006) 2931.
[24] A. Trkov, G.L. Molnár, Z. Révay, S.F. Mughabghab, R.B. Firestone, V.G. Pronyaev, A.L. Nichols, M.C. Moxon, Nucl. Sci. Eng. 150 (2005) 336.
[25] A.E. Waltar, A.B. Reynolds, Fast Breeder Reactors, Pergamon, New York, USA, 1982.
[26] R. Manzel, C.T. Walker, J. Nucl. Mater. 301 (2002) 170.
[27] H.U. Zwicky, E.T. Aerne, A. Hermann, H.A. Thomi, M. Lippens, J. Nucl. Mater. 202 (1993) 65.
[28] G. Bart, O. Gebhardt, E.T. Aerne, M. Martin, in: Proceedings of IAEA Technical Committee Meeting on Development of Post-Irradiation Examination at the Reactor Fuel Examination Facility, Cadarache, France, 17–21 October 1994, IAEA-TECDOC-822, 1995, p. 337.

[29] J. Basselier, T. Maldague, M. Lippens, in: P. Chantoin (Ed.), Proceedings of IAEA Technical Committee Meeting on Recycling of Plutonium and Uranium in Water Reactor Fuel, Newby Bridge, Windermere, UK, 3–7 July 1995, IAEA-TECDOC-941, 1997, p. 277.
[30] M. Lippens, T. Maldague, J. Basselier, D. Boulanger, L. Mertens, in: V. Onoufriev (Ed.), Proceedings of Symposium on MOX Fuel Cycle Technologies for Medium and Long Term Deployment, IAEA – OECD/NEA, Vienna, Austria, 17–21 May 1999, CSP-3/P, p. 220.
[31] S.B. Fisher, R.J. White, P.M.A. Cook, S. Bremier, R.C. Corcoran, R. Stratton, C.T. Walker, P.K. Ivison, I.D. Palmer, J. Nucl. Mater. 306 (2002) 153.
[32] F.N. Kryukov, G.D. Lyadov, O.N. Nikitin, V.P. Smirnov, A.P. Chetverikov, Atom. Energy 100 (2006) 1.
[33] R. Weston, I.D. Palmer, G.M. Wright, G.D. Rossiter, R.C. Corcoran, T.C. Gilmour, C.T. Walker, S. Bremier, in: Proceedings of ENS International Topical Meeting – Nuclear Fuel: Development to Meet the Challenge of a Changing Market, Stockholm, 27–30 May, p. P2.
[34] R.J. White, S.B. Fisher, P.M.A. Cook, R. Stratton, C.T. Walker, I.D. Palmer, J. Nucl. Mater. 288 (2001) 43.
[35] C.T. Walker, W. Goll, T. Matsumura, J. Nucl. Mater. 228 (1996) 8.
[36] F. Sontheimer, H. Landskron, in: V. Onoufriev (Ed.), Proceedings of IAEA Technical Committee Meeting on Nuclear Fuel Behaviour Modelling at High Burnup, Lake Windermere, UK, 19–23 June 2000, IAEA-TECDOC-1233, 2001, p. 105.
[37] R. Manzel, C.T. Walker, in: Proceedings of Topical Meeting on LWR Fuel Performance (Oral Session), American Nuclear Society, Park City, Utah, USA, 10–13 April 2000, p. 604.
[38] J. Killeen, J.A. Turnbull, E. Sartori, in: Proceedings of International LWR Fuel Performance Meeting, American Nuclear Society, San Francisco, California, USA, 30 September–3 October 2007, p. 261.
[39] P. Menut, E. Sartori, J.T. Turnbull, in: Proceedings of Topical Meeting on LWR Fuel Performance (Poster Session), American Nuclear Society, Park City, Utah, 10–13 April 2000, p. 325 (data available at OECD/NEA: <http://www.nea.fr/html/science/fuel/ifpelst.html>).